Macromolecules

ARTICLE

pubs.acs.org/Macromolecules

Common Origin of Dynamics Heterogeneity and Cooperatively Rearranging Region in Polymer Melts

Makoto Asai,*[,†] Mitsuhiro Shibayama,[†] and Yasuhiro Koike[‡,§]

[†]The Institute for Solid State Physics, The University of Tokyo, 5-1-5, Kashiwanoha, Kashiwa, Chiba 277-8581, Japan

[‡]Faculty of Science and Technology, Keio University, 3-14-1, Hiyoshi, Kohokuku, Yokohama, Kanagawa, 223-8522, Japan

[§]Keio Photonics Research Institute, Keio University, 7-1, Shinkawasaki, Saiwai-ku, Kawasaki, Kanagawa, 212-0032, Japan

ABSTRACT:

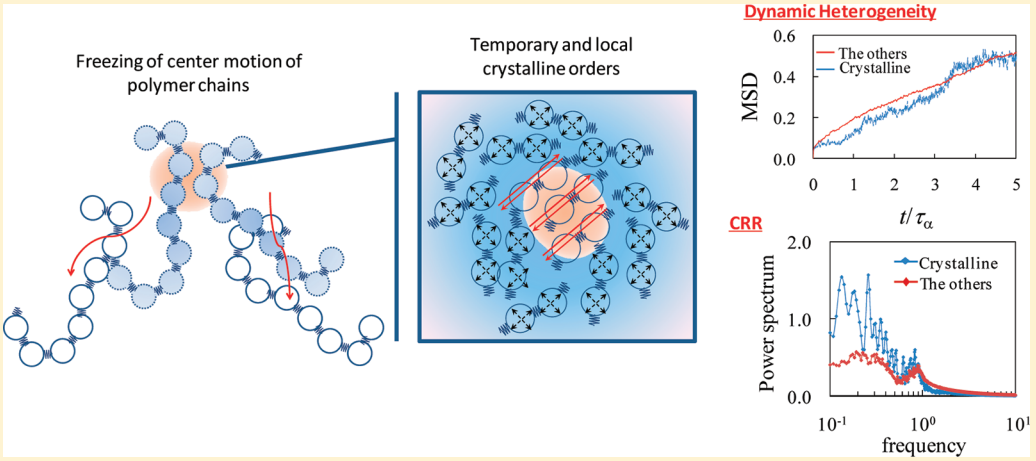

If some supercooled liquids are cooled further, they freeze into a specific medium state with both properties of liquid-like structure and solid-like hardness, so-called "glass." The fact that dynamics freeze drastically when there is only a slight change in static structure remains a mystery in solid-state physics. Recently, it has been reported that when a particular kind of glass-forming liquids with two order parameters are cooled rapidly, local crystalline orders with extremely slow dynamics start to emerge when approaching glass transition temperature. This result suggests a concept of "frustration to crystallization" as a physical picture of glass transition. On the other hand, although Adam−Gibbs theory has predicted the existence of cooperatively rearranging region (CRR) as the origin of extreme slowdown in dynamics, CRR is still no more than a hypothetical subsistent to explain the slow dynamics of glass transition. In this study, we found for the first time, local-bond orientational orders, "LBOOs," which characterize glass transition in polymer melts, one of the most representative glass-forming liquids. Furthermore, we confirmed that monomers composed of LBOOs were concertedly vibrating and indicated that LBOOs can be identified as CRR. In other words, we were able to prove that the LBOOs we have discovered were consistent with both the physical picture of frustration to crystallization and Adam−Gibbs' theory.

1. INTRODUCTION

If supercooled liquids are cooled further, they freeze into a specific medium state with both properties of liquid-like structure and solid-like hardness, so-called "glass."[1,2] The principal mechanism of this phenomenon, known as glass transition, is one of the most difficult and challenging issues in solid-state physics and still remain as a mystery.[3−5] Generally, when a phase transition such as liquid−solid transition occurs, the long-distance order parameter appears. In glass transition, however, such order parameter cannot be confirmed and liquid-like static disordered structure remains spread throughout. In other words, even though static structure changes slightly, the dynamics freeze drastically.[3−6] Many theoretical[7−10] and experimental[11−14] works have been made in approach to find this "hidden order parameter" in glass state. Free-volume theory,[15] mode-coupling theory,[16] energy-landscape theory,[2,17] and spin-glass model[18] are few examples of such works that have attempted to explain glass transition, yet had not grasped the complete concept. Over the years, researches concerning glass-transition have greatly advanced with the establishment of computer simulations. The molecular dynamic approach,[19−21] distinct for its ability to analyze the movement of each particle in detail, is one field that has advanced with computer simulation. Data obtained by simulation are extremely difficult to obtain by experiment. This applies to studies of glass-transition as well, and thus simulation plays a critical role in its investigation. Recently, by computer simulations of Lennard-Jones (LJ) liquids with anisotropic potential[22] and polydisperse two-dimensional colloidal glass,[23]

Received: June 15, 2011
Revised: July 25, 2011
Published: August 02, 2011

a split in a short-distance peak of radial distribution function $g(r)$ around the glass transition temperature T_g has been confirmed. This split has been indicated as a subtle structural change characterizing glass state. Moreover, medium range crystalline order (MRCO), which corresponds to this change in $g(r)$, has also been found. These local crystalline structures identify dynamic heterogeneity, which are caused by frustration toward the most stable state.[22,23]

It should be noted, however, that these crystalline structures occur in glass forming liquids as like colloids and has never yet been reported about occurring in polymer glass, despite that it is one of the most typical glass-forming materials. Experimental results indicate possibility that dynamic heterogeneity exists in polymer glass.[24] Thus, the unavoidable question arises. If dynamic heterogeneity is indeed correlated with MRCO, would not it be easily found in polymer glass? Why is it that crystalline structures cannot be found neither by simulation or experiment? We think that the answers to these questions lie in the fact that MRCO cannot be found in Å ordered-space scale. We believe that if we observe polymer glass from the right perspective, we will be able to find these structures, and that this "right perspective" is if we observe it in a space scale in which a polymer chain can be coarse-grained as a Gaussian chain. Polymer chains can be interpreted this way because of the conformation limitation of chemical bonds between neighbor monomer units.

To verify this new hypothesis, and find correlation between dynamic heterogeneity and MRCO, we regard polymer as a form of Kremer−Grest model (bead−spring model).[25] Provided by the fact that polymer chain is long enough to be regarded as a Gaussian chain with entropic elasticity and further divided into Gaussian chains consisting of several monomers, the structure and dynamics of straight-chain polymer can be regarded as this coarse grained model. Here, each Gaussian chain and its entropic elasticity correspond to the bead and spring, respectively. In this coarse grained scale, straight-chain polymers act relatively similar to simple LJ liquids. The only difference is the springs potential between neighboring beads within the same chain.

The Kremer-Grest model has proven to indicate universal scaling between structural relaxation and vibration dynamics for glass-forming liquids and polymers.[26] By applying molecular dynamics, an effective method to investigate microscopic dynamics of molecules, to the bead spring model, we will not only be able to find MRCO, but also reveal the correlation between MRCO and dynamic heterogeneity to discover the universal origin of slow dynamics in glass state.

2. MODEL AND SIMULATION TECHNIQUE

There are mainly two methods to investigate glass-transition of polymers by molecular dynamics simulation.

The first method is to use a model that regards polymers in atomic scales. This method takes into account the chemical structure in the calculation, which allows the prediction of the absolute value of T_g of materials. However, the typical integration time step is about δt = 1.0 fs, and requires immense calculation, about an order of 10^8 to calculate 100 ns. Considering that we can only observe glass transition in this model for only a few seconds at laboratory level, this model is unfit to completely grasp the concept of glass-transition. Thus, it becomes most effective to use coarse-grain method.

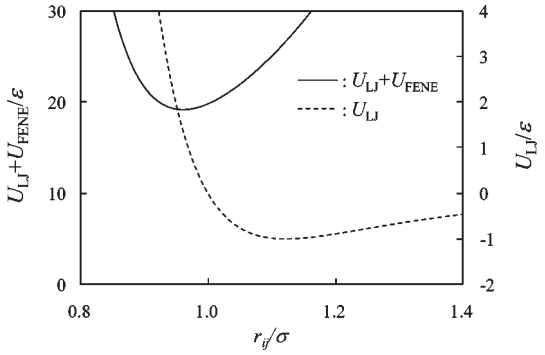

Figure 1. Potential energy of Kremer−Grest model.

As already mentioned, the most famous coarse grained model of polymers is the bead spring model proposed by Kremer et al., a model known to vitrify without crystallization.[27] Generally, when a model is coarse-grained, minute information on its chemical structure is lost. However, since glass-transition is a universal phenomenon, it is possible to discuss general characteristics of glass transition by this method. With the coarse-grained scale, we believe that polymers can be perceived as a dynamic system very similar to that of colloids and LJ liquids. Thus, we expect to find MRCO as observed in LJ liquids.

In the present work, our investigated combinations of polymer chain number p and segment number n of a polymer chain are 20 and 400, respectively. Total segment number N is 8000. All segments mass m_i are set to 1.0. Polymer segments are soft spheres, which have a diameter of σ and are bonded by a finitely extensible nonlinear elastic (FENE) potential:

$$U^F(r) = \frac{1}{2}kr_0^2 \ln\left[1-\left(\frac{r}{r_0}\right)^2\right], \quad r_0 = 1.5\sigma,\ k = 30 \qquad (1)$$

Here, r is the distance between neighbor polymer segments in same polymer chain in units of σ, T is the temperature in units of ε/k_B, r_0 is the limitation length of a spring in units of σ, and k is the spring coefficient. Moreover, the interaction between i and j monomers is Lennard-Jones potential

$$U^{LJ}(r) = 4\varepsilon\left[\left(\frac{r}{r_{ij}}\right)^{12} - \left(\frac{r}{r_{ij}}\right)^{6}\right] + c,\ r \le r_{\text{cutoff}} = 4.5\sigma \qquad (2)$$

where r_{ij} is the distance between i and j monomers in units of σ and ε is the well depth of the potential. LJ potential is minimum ($r_{\min}$) at $r = 2^{1/6}\sigma$. We define the cutoff distance as r_{cutoff} =4.5σ, and constant c = 0.00048 when $U^{LJ}(r{=}r_{\text{cutoff}})$=0. In the present work, we chose σ = 1 and k_B = 1. The superposition of FENE and LJ potentials leads to a minimum position $b_{\min}$. Note that there exists two stabilization points $r_{\min}$ and $b_{\min}$ in this polymer model. As shown in Figure 1, $b_{\min}$ is 0.96 and $r_{\min} = 2^{1/6}$ ($\approx$1.12). In other words, when one simplifies the potential energy that acts upon coarse-grained polymers, one begins to see that fundamentally, there exists two stabilization points in polymers. Such structure with several stabilization points is typically known to cause frustration in its system.

Prof. Tanaka's group observes MRCO by providing frustration to the system. Frustration is provided by artificially introducing

anisotropic potential or dispersion in particle diameter when vitrifying LJ liquid and colloidal liquid.[22,23] However, in a coarse grained model, it is unnecessary to artificially apply frustration because it is generated naturally, a point which we found worth noting. This model has been studied from various perspectives, such as the dependence of T_g on cooling rate,[28] validation of mode-coupling,[29−31] the dynamics of glass state and its relation to Rouse mode,[32] and studies on dynamic heterogeneities.[33] Yet none of these studies have reported anything concerning MRCO.

Next, we will explain the two simulation techniques used in this study. The first is boundary conditions set on the simulation cell. Generally, the magnitude that computer simulation could withstand is about 10^4∼10^5 particles, due to its limitation in performance. However, in reality, matter is made up of particles in order of 10^{23}, which is 10^{20} greater than that calculated by simulation. Typically, such difference is creatively compensated by imposing periodic boundary conditions on the computer cell. By this calculation method, the dynamics observed within the simulation cell is apt to represent dynamics of the entire system. The second technique is the control method of temperature and pressure. In this study, we used the Nosè thermostat[34,35] and Andersen barostat[36] to calculate molecular dynamics under constant temperature and pressure (*NPT* ensemble). The motion equation is written as follows.

$$\ddot{\xi}_i = -\frac{1}{m_i V^{2/3}}\frac{\partial U}{\partial \xi_i} - \frac{2}{3}\frac{\dot{V}}{V}\dot{\xi}_i - \frac{\dot{s}}{s}\dot{\xi}_i \tag{3}$$

$$\xi_i \equiv V^{-1/3}\dot{\mathbf{r}}_i, \quad 0 \le \xi_i \le 1,$$

$$\ddot{s} = \frac{2s}{Q}\left(\sum_{i=1}^{N}\frac{m_i}{2}\dot{\mathbf{r}}_i^2 - \frac{3}{2}Nk_B T_0\right) + \frac{\dot{s}^2}{s}, \tag{4}$$

$$\ddot{V} = \frac{s^2}{W}\left(\frac{1}{3V}\sum_{i=1}^{N} m_i\dot{\mathbf{r}}_i^2 - \frac{1}{3V}\sum_{i=1}^{N}\frac{\partial U}{\partial \mathbf{r}_i}\cdot\mathbf{r}_i - P_0\right) + \frac{\dot{s}^2}{s}\dot{V} \tag{5}$$

Here V is the volume of the simulation cell, U is the potential of the system, $\mathbf{r}_i$ is the position vector of segment i, $\boldsymbol{\xi}_i$ is the scaled position vector of segment i, Q is the inertial parameter of heat source parameter s, g is the total number of degrees of freedom in the system, W is the inertial parameter of a piston, T_0 is the preset temperature and P_0 is the preset pressure. Time t, and pressure P are in units of $(m_i\sigma^2/\varepsilon)^{1/2}$, and ε/σ^2, respectively. Nosè−Andersen Hamiltonian H is expressed by

$$\mathrm{H} = \sum_{i=1}^{N}\frac{1}{2}m_i V^{2/3}\xi_i^2 + U(V^{1/3}\xi^N) + \frac{Q}{2s^2}\dot{s}^2 + gk_B\ln s + \frac{W}{2s^2}\dot{V}^2 + P_0 V \tag{6}$$

By placing $\boldsymbol{\xi}_i$, V, and s on a general coordinate system, and resolving eq 3, 4, and 5, it becomes possible to control the temperature and pressure of the system, T_0 and P_0, respectively, to a desired value. A stepwise cooling in steps of $\Delta T = 0.1$ starting from $T = 1.0$ to $T = 0.2$ was carried out, using cooling rate of $\Gamma = 10^{-6}$ (in MD time units) defined as $\Gamma = \Delta T/\Delta t$. Here, Δt is 100000 MD time steps (one MD time steps corresponds to $t = 0.006(m_i\sigma^2/\varepsilon)^{1/2}$).

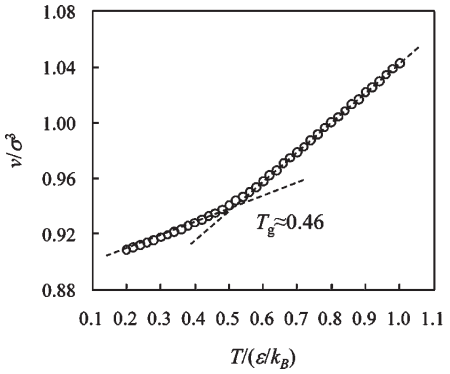

Figure 2. *T*-dependence of *v*.

3. RESULTS AND DISCUSSION

3.1. Glass Transition Temperature. To fully understand the dynamics of glass transition, we must first define the glass transition temperature T_g. Generally, the T-dependence of specific volume v changes below and above T_g, because all particles are frozen and immobilized below T_g. Therefore, T_g can be defined as the point at which the slope of T-dependence of v changes, which is shown in Figure 2. From this result, we determined T_g as $T = 0.46$.

3.2. Dynamic Heterogeneity. The dynamics of polymer used in this study is well portrayed in Figure 3. In Figure 3a, the dynamic heterogeneity is observed by self-part intermediate scattering function (ISF). It is calculated as follows:

$$F(\mathbf{q}, t) = \frac{1}{N}\sum_i \exp[j\mathbf{q}\cdot(\mathbf{r}_i(t) - \mathbf{r}_i(0))] \tag{7}$$

Here N is the number of all polymer segments and $\boldsymbol{q}$ is the wavenumber corresponding to the first peak of the structure factor. The structural relaxation that shows long-time decay in ISF is called α relaxation, and can be fitted by a stretched exponent function (the empirical Kohlrausch−Williams−Watts formula): $\exp[-(t/\tau_\alpha)^\beta]$, where relaxation time of α mode (α relaxation) τ_α is defined as $F(\boldsymbol{q}, \tau_\alpha) = 1/e$, and β is the stretching parameter. In the range of $T = 1.0$ to $T = 0.7$, a stretched exponential well fits $F(\boldsymbol{q}, t)$. Note that a plateau region appears at $T \approx 0.6$, which indicates that there are two-steps in relaxation process ("fast β" and "α relaxation"). In other words, dynamic heterogeneity starts to appear when approaching T_g. The relaxation occurring at the plateau region is called the Johali−Goldstein process. To better understand the nature of the polymer used, we observe the $1/T$-dependence of τ_α (Angell plot) as shown in Figure 3(b). Generally, in glass-forming liquids, it is well-known that τ_α is fitted by the Vogel−Fulcher−Tammann (VFT) equation[37−39]

$$\tau_\alpha = \exp\left[\frac{D}{T - T_0}\right] \tag{8}$$

where D is fragility index and T_0 is ideal glass transition temperature. Although Hecksher has recently concluded that VFT is not necessarily the most adequate equation to be used as the fitting function,[40] our data are fitted by VFT equation to determine whether the T-dependence of τ_α in the polymer systems used is Arrhenius or non-Arrhenius. As fitting parameters, we determined T_0 and D to be 0.31 and 1.72, respectively. As shown in the Figure, $1/T$-dependence of τ_α can indeed be

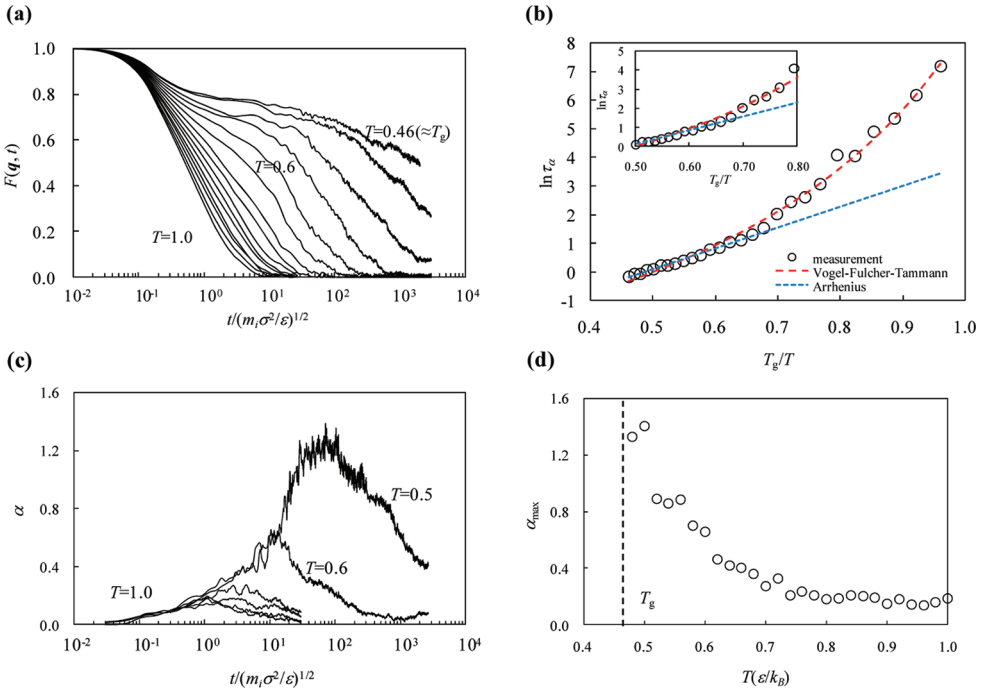

Figure 3. Dynamic heterogeneity. (a) t-dependence of $F(\boldsymbol{q}, t)$. (b) $\ln\tau_\alpha$ versus T_g/T (Angell plot). Solid lines represent VFT equation. Dashed line represents Arrhenius equation: $\tau_\alpha=\tau_0 \exp[E/T]$, where E is activation energy. Inset: Closer focus of shift point from Arrhenius to VFT. (c) t-dependence of α. (d) T-dependence of α_{max}.

fitted by VFT equation and determined as Arrhenius in the region of high temperature. However, note that as T approaches T_g, its difference with the Arrhenius equation dramatically increases.

We take another close look at dynamic heterogeneity in Figure 3, parts c and d. The glass state is considered a system with nonergodic property in which non-Gaussianity appears.[41−43] In this state, dynamic heterogeneity is known to occur. Figure 3c shows the time dependence of the non-Gaussian parameter (NGP), which is expressed by

$$\alpha(t) = \left\langle \frac{3\Delta\mathbf{r}_i(t)^4}{5(\Delta\mathbf{r}_i(t)^2)^2} - 1 \right\rangle \tag{9}$$

Here, the bracket denotes an ensemble average. As it is obviously seen, the peak of NGP shifts to a longer time with decrease of T. Figure 3(d) shows T-dependence of maximum α_{max} of NGP. Note that α_{max} increases drastically below $T \approx 0.6$.

3.3. Local-Bond Orientational Orders. In earlier discussion, we observed dynamic heterogeneity around T_g in polymer system. It is noted that dynamic heterogeneity appears prominently around $T\approx0.6$. (This temperature will be discussed in section 3.6) Next, we investigated whether some kind of ordered structures are associated with glass transition. It is unlikely that icosahedral structures are formed, because each segment is chemically bound with neighboring segments within same chain unlike colloid and LJ liquid. Instead, it is intuitively plausible that ordered structure such as locally bundled bonds exists. We call these "Local-bond-orientational-orders (LBOOs)." Hence, we define the bonds correlation function $\psi(L, \theta)$ to detect LBOOs as follows:

$$\psi(L,\theta) = \frac{\langle\phi_i(L,\theta)\rangle}{\sin\theta \int \langle\phi_i(L,\theta)\rangle \, d\theta}, \quad 0 \le \theta \le 90^\circ \tag{10}$$

Here, L is the distance between midpoints of any two bonds, θ is the angle between the any two bonds, $\phi_i(L,\theta)$ is measured number of segments which has the angle $\theta \sim \theta + \Delta\theta$ and the distance L with segment i, and the bracket denotes an ensemble average. We set $\Delta\theta$ to 0.5 deg (see Appendix). When L is large enough, in other words, when two bonds are not correlated, $\psi(L,\theta)$ becomes 1.0. If two bonds are correlated, $\psi(L,\theta)$ becomes greater than 1.0. Figure 4 shows T and L-dependence of $\psi(L,\theta)$. As it can be seen, when L = 5.0, $\psi(L,\theta)$ is almost 1.0. This indicates that two bonds are displaced far enough and are not correlated at any temperature. In smaller L, same tendency in T and L-dependence of $\psi(L,\theta)$ is observed. Same trend continues from L = 5.0 to L = 1.3, but at smaller L, a large change is observed. When L = 1.1 and 1.2, $\psi(L,\theta)$ has a sharp peak at θ = 0−5 deg, and it corresponds to LBOOs. This is likely due to the fact that the two bonds are oriented. When the distance between the two bonds become no less than that of neighboring segments (corresponding to r_{min}, or see the position of first peak shown in Figure 6a), the neighboring bonds connected to each bond cause steric-hindrance. Thus, the two bonds become oriented. It should be noted that this peak increases to twice its height under T_g. These results indicate that LBOOs drastically appear around T_g.

In addition, it is found that up to three bonds can be directed parallel to a bond in our system. In order for us to identify which LBOOs are connected with glass transition, we broke down T-dependence of number of segments into LBOOs composed of two bonds and those composed of three or four bonds. It should be noted that we calculate time average of 10000 MD time steps as number of segments because LBOOs fluctuate over time. The number of segments of LBOOs composed of two bonds and that of three or four bonds are $\langle N_{p1}\rangle$ and $\langle N_{p2,3}\rangle$, respectively. T-dependence of $\langle N_{p1}\rangle$ and $\langle N_{p2,3}\rangle$ are shown in Figure 5, parts a and b, respectively. $\langle N_{p1}\rangle$ is inversely proportional to T. On the

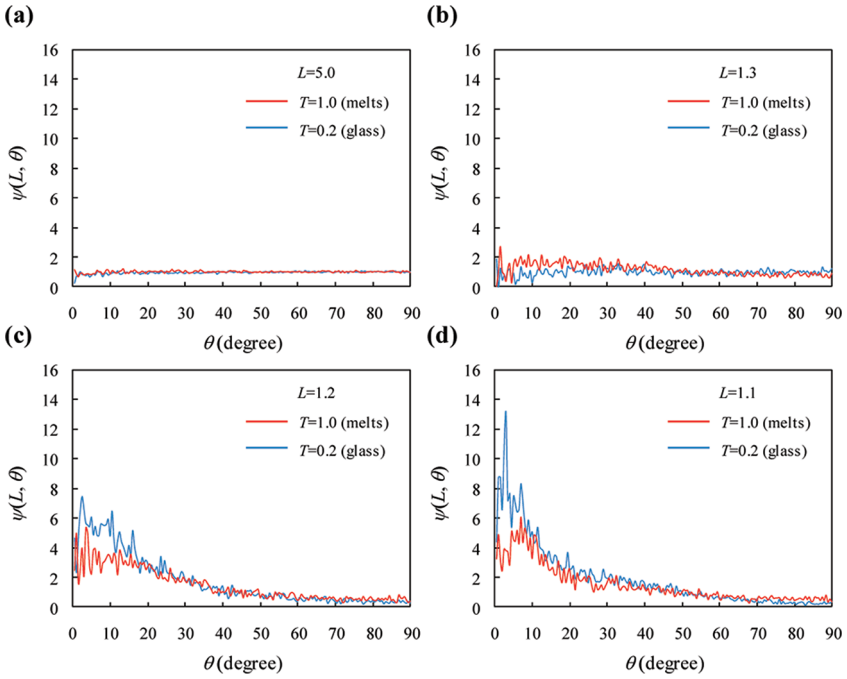

Figure 4. T-dependence of $\psi(L, \theta)$. Red line and blue line represent $T = 1.0$ (melts) and $T = 0.2$ (glass), respectively: (a) $L = 5.0$; (b) $L = 1.3$; (c) $L = 1.2$; (d) $L = 1.1$.

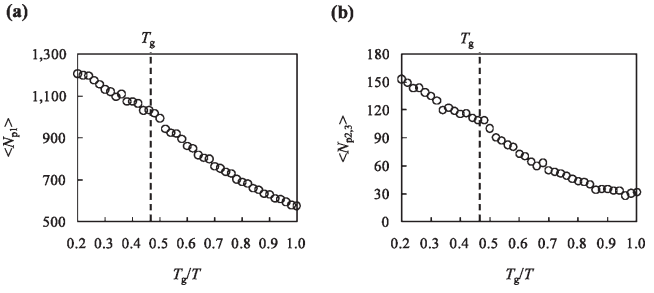

Figure 5. T-dependence of the number of segments composed of LBOOs: (a) $\langle N_{p1} \rangle$; (b) $\langle N_{p2,3} \rangle$.

other hand, even though $\langle N_{p2,3} \rangle$ is nearly unchanged from $T = 1.0$ to $T = 0.86$, in further low temperatures, $\langle N_{p2,3} \rangle$ increases with decrease of T. Especially, from $T = 0.86$ to $T = 0.48(\approx T_g)$, it increases drastically. From this analysis, we judged that LBOOs composed of over two bonds are strongly correlated with glass transition and will further refer to these specific LBOOs when we mention "LBOOs" hereafter.

3.4. Radial Distribution Function. Next, we investigate the radial distribution function $g(r)$, defined as

$$g(r) = \frac{1}{4\pi r^2 \rho \Delta r} \left\langle \sum_{i=1}^{N} n_i(r) \right\rangle \tag{11}$$

where ρ is the density, and $n_i(r)$ is the number of segments between r and $r + \Delta r$. We chose $\Delta r = 0.005$. Figure 6a shows a wider region of $g(r)$. There are two close peaks at around $r = 1.0$, so-called "first peak". These peaks correspond to the equilibrium position (the cage position) of neighboring segments interacted by only LJ potential and both of LJ potential and FENE potential, respectively. The former position is $r \approx 1.12$ $(=r_{min})$, and the later is $r \approx 0.97$ $(=b_{min})$. Notice the first peak changed into two

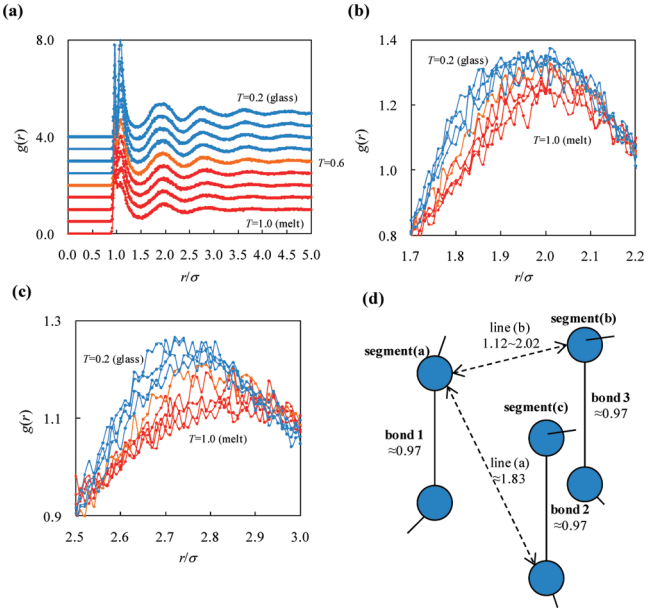

Figure 6. T-dependence of $g(r)$. (a) Bule lines are blow T_g (glass state). Orange lines are $T = 0.60$. Red lines are otherwise. (b) Closer focus of second peak around $r = 2.0$. (c) Closer focus of third peak around $r = 3.7$. (d) Pattern diagram represents typical configuration of LBOOs.

sharp peaks from two gentle peaks with decrease of T due to decrease of thermal vibration of segments.

Figure 6b focuses on the range of $1.7 \leq r \leq 2.2$ of $g(r)$, corresponding to the "second peak". When decreasing T from 1.0 to 0.7, the second peak remains unchanged. However, below $T \approx 0.6$, the top of the second peak increases and the peak broadens at smaller range of the peak $(1.7 \leq r \leq 2.0)$. The pattern diagram of LBOOs configuration which causes these

dx.doi.org/10.1021/ma201341d |*Macromolecules* 2011, 44, 6615–6624

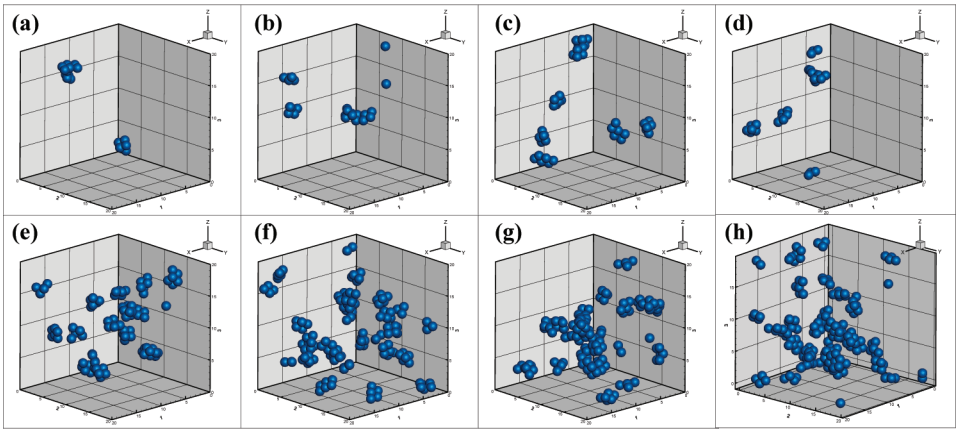

Figure 7. Snapshots of LBOOs. Square boxes are simulation cell. Key: (a) $T = 1.0$; (b) $T = 0.9$; (c) $T = 0.8$; (d) $T = 0.7$; (e) $T = 0.6$; (f) $T = 0.5$ ($\approx T_g$); (g) $T = 0.4$; (h) $T = 0.2$.

changes is shown in Figure 6d. When two bonds (bond 1, bond 2) are oriented and four segments composed of two bonds are lined up in form of parallelogram, the length of line a is 1.83 and it corresponds to broadening of the second peak around $r = 1.8$. Given that bond 3 is directed parallel to bond 2, the length of line b varies depending on the position of bond 3. When three bonds are coplanar, the length of line b is a maximum of 2.02. When the triangle formed by segments a−c is an equilateral triangle, line b is a minimum of 1.12. These values imply that bond 3 causes the broadening of the second peak.

Figure 6c shows the range of $2.5 \leq r \leq 3.0$ of $g(r)$, corresponding to the "third peak". When decreasing T from 1.0 to 0.7, the third peak remains unchanged. However, below $T \approx 0.6$, the top of the third peak increases and the position of the peak shifts to 2.70 from 2.90. Similar to the case of the second peak, given that bond 4 is directed parallel to bond 3, the length of line c can be estimated as 2.70.

A snapshot of LBOOs is shown in Figure 7. We identify segments composed of bonds which apply the conditions of $0 \leq \theta \leq 5$ at $1.0 < L \leq 1.2$ as LBOOs. Although only few LBOOs are found above $T = 0.7$, they rapidly appear at lower temperatures. This result agrees well with the result of T-dependence of $\langle N_{p2,3} \rangle$ shown in Figure 5b. Further note that LBOOs are not suspended, but localized. In other words, the correlation length of LBOOs becomes longer with decrease of T.

3.5. Correlation Between Dynamic Heterogeneity and Orientational Bond Orders. We have made clear that both dynamic heterogeneity and LBOOs emerge in association with glass transition. We then investigated if there are any correlation between LBOOs and dynamic heterogeneity. We compared mean-square-displacement (MSD) of segments composed of LBOOs with that of other segments. MSD is calculated as $\langle \Delta \boldsymbol{r}(t)^2 \rangle$. Figure 8 shows time changes of MSD at $T = 0.66$, 0.60, 0.56, and 0.50. Blue lines and red lines are MSD of LBOOs and others, respectively. Time axes are normalized by relaxation time τ_α of each temperature condition. When $T = 0.66$, there is little to distinguish LBOOs from others in all time range. However, when $T = 0.6$, notable difference appears. MSD of LBOOs is obviously smaller than that of the others and this trend continues from short to long time frame. This difference between MSD of both is dynamic heterogeneity and this result obviously indicates that LBOOs are correlated with dynamic heterogeneity. Moreover, MSD at short time frame τ_β ($t \approx 1.0$) is called the "Debye−Waller factor" and expressed as $\langle \Delta \boldsymbol{r}(\tau_\beta)^2 \rangle$. This factor represents the size of the cage and is negatively correlated to the system's solidity.[26] Thus, it can be seen that LBOOs have far more solidity than others. Also note that this trend continues to approximately three times τ_α and after that, the differences disappear. This result indicates that the lifetime of LBOOs is approximately three times τ_α. Same results are observed in cases of $T = 0.56$ and 0.50 ($\approx T_g$). In conclusion, our studies indicate that LBOOs are correlated with dynamic heterogeneity. This correlation strongly indicates possibility that LBOOs are the origin of dynamic heterogeneity and eventually slows the dynamics in glass transition.

3.6. Motion of Center of Polymer Chains. We confirmed that dynamic heterogeneity and LBOOs were found in association with glass transition. In both cases, characteristic changes were observed around $T \approx 0.6$, which was higher than glass transition temperature. Therefore, we investigate whether this temperature is physically meaningful. In our system, the melting temperature T_m has been reported as $T_m \approx 0.76$.[28] $T \approx 0.6$ is roughly midpoint between T_m and T_g. In polymer, "rubber state" is defined as a state where cross points of polymer chains become fixed, and diffusion of polymer chain is frozen. Although cross points are fixed, the polymer chains still have mobility, which is a distinguishing feature of this state. We predict that a characteristic temperature, in which polymer chains are frozen, exists between T_m and T_g. We call this temperature as rubber transition temperature T_r.

The diffusion of polymer chain can be calculated as the diffusion of its center. The center position of the polymer chain is defined as $\boldsymbol{r}_G(t) = 1/n\Sigma \boldsymbol{r}_i(t)$, where $\boldsymbol{r}_i(t)$ is position vectors of polymer segment i, and t is time. The differential MSD of the center of the polymer chain is calculated as $d\langle \Delta \boldsymbol{r}_G(t)^2 \rangle / dt$. It is known that MSD of all segments composed of polymer chains goes through four stages. At the first stage, polymer chains behave free from the tube of reptation theory and operate in accordance with Rouse mode. Therefore, MSD of all polymer segments is proportionate to $t^{1/2}$. At the second stage, the motion of polymer chains becomes subject to the restriction of the tube, and then polymer chains move one-dimensionally along the tube. Hence, MSD is proportionate to $t^{1/4}$ and then, $t^{1/2}$. After that, polymer chains are thrown off the limitation of the tube and MSD is proportionate to t^1. We calculated MSD of center of polymer chains in the time-range, in which MSD of all segments

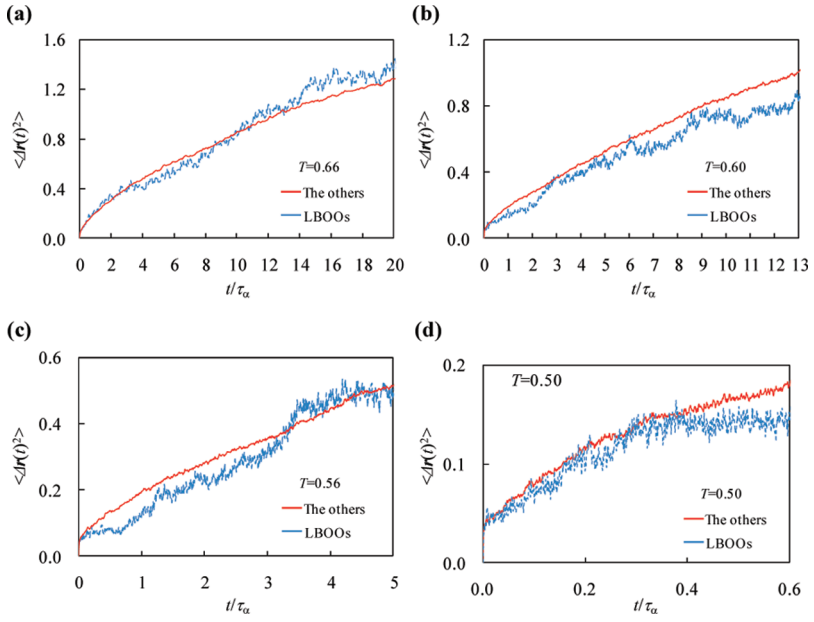

Figure 8. *t*-Dependence of MSD. Blue line and red line represent segments composed of LBOOs and the others, respectively: (a) $T = 0.66$; (b) $T = 0.60$; (c) $T = 0.56$; (d) $T = 0.50$.

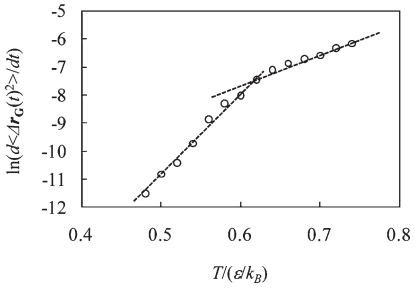

Figure 9. T-dependence of $d\langle \Delta \boldsymbol{r}_G(t)^2 \rangle / dt$.

is proportionate to $t^{1/2}$ at the second stage to observe that the motion of polymer chains is frozen in the tube. Figure 9 shows T-dependence of $d\langle \Delta \boldsymbol{r}_G(t)^2 \rangle / dt$. Note that $d\langle \Delta \boldsymbol{r}_G(t)^2 \rangle / dt$ decreases with decrease of T, and falls abruptly around $T \approx 0.6$. We define T_r as the point at which the slope of T-dependence of $d\langle \Delta \boldsymbol{r}_G(t)^2 \rangle / dt$ changes. From this result, we determined T_r as 0.61. This temperature agrees well with the temperature in which dynamic heterogeneity and LBOOs drastically emerges. This means that we can interpret this as follows: In a temperature in which the motion of center of polymer chains is active enough, it is very difficult to form LBOOs because segments have translatory motion component. However, with decrease of temperature, LBOOs are formed and thus this slows down the center-of-mass motion. Furthermore, when LBOOs are formed, the center-of-mass motion is further slowed down, and induces formation of more LBOOs. From this cycle of reactions, dynamics heterogeneity begins to emerge. In other words, in polymer system, T_r is a motive temperature in which LBOOs and dynamic heterogeneity start to emerge.

3.7. Cooperatively Rearranging Region. Conventionally, in Adam−Gibbs' theory,[44] the slow dynamics of glass transition can be explained by the presence of Cooperatively Rearranging Region (CRR). However, it still remains a mystery why CRR emerges when approaching glass transition. CRR is still no more than a hypothetical subsistent to explain the slow dynamics of glass transition. On the other hand, in this study, we confirmed the strong correlation between LBOOs and dynamic heterogeneity. Given these facts, it stands to reason that LBOOs are both structural orders and dynamic orders, the so-called "CRR". Therefore, we calculate velocity autocorrelation function $C_u(t)$ as follows,

$$C_u(t) = \frac{\langle \mathbf{v}_i(t) \cdot \mathbf{v}_i(0) \rangle}{\langle \mathbf{v}_i(0)^2 \rangle} \tag{12}$$

Here, $\boldsymbol{v}_i(t)$ is a velocity vector of segment i, and the bracket denotes an ensemble average. The range of measurement time is $0 \le t \le 2\tau_\alpha$. We compute Fourier transformation to the obtained $C_u(t)$ to analyze differences between LBOOs and the others in vibrational component of segments. Figure 10 shows power spectrum at $T = 0.60$, 0.56, 0.52, and 0.46. Blue lines and red lines are LBOOs and the others, respectively. In both power spectra, there are two vibrational components: one is thermal oscillation at high frequency region, and the other is spring oscillation at low frequency region, which is caused by entropic elasticity. However, whereas there is a broad spectrum of high frequency component originating from thermal noise in the spectrum of the segments other than LBOOs, there is not such high frequency component in that of LBOOs (see insets). Moreover, the peak of thermal oscillation at high frequency region decreases when approaching T_g, while the peak caused by spring vibration increases. This result can be interpreted that spring vibration is the more dominant vibration for LBOOs than the other segments, and the segments composed of LBOOs are concertedly vibrating in the direction of the orientational bond.

The purpose of this study is to investigate whether or not LBOOs could be identified as CRR. From analysis of vibration spectra, it is clear that LBOOs vibrate concertedly. Also note that this concerted vibration continues on to until $t \approx 2\tau_\alpha$. In other words, we can interpret that LBOOs vibrate concertedly within the time frame of Debye−Waller region to its lifetime, which is

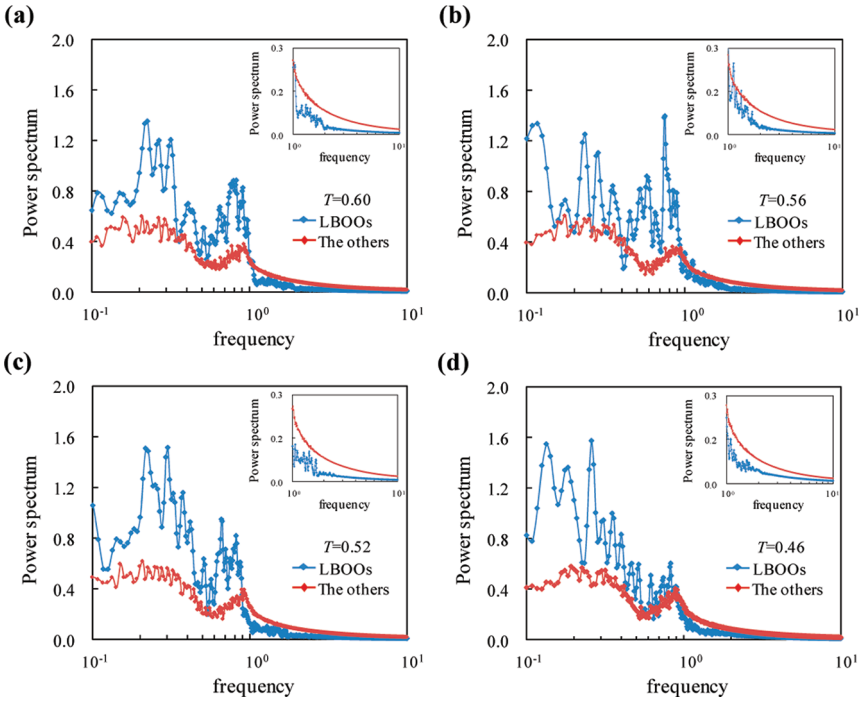

Figure 10. Power spectrum of segments vibration. Blue line and red line represent segments composed of LBOOs and the others, respectively. Key: (a) T = 0.60; (b) T = 0.56; (c) T = 0.52; (d) T = 0.46. Inset: Closer focus of high frequency region.

the time frame of diffusion motion. If CRR consists of segments in crystalline order, then it is natural to assume that this region vibrates concertedly. On the basis of this assumption and observation of LBOO behavior, it is possible to think that the concerted vibration of CRR is equal to concerted vibration of LBOOs. Thus, LBOOs that we have discovered may be a possible candidate for CRR in polymer glass.

4. CONCLUSION

By simplifying polymer by coarse-graining, we investigated the ordering process underlying glass transition. Using bonds correlation function, we were able to find local crystalline orders, "LBOOs", which characterized glass transition, and revealed their structure. We also confirmed that LBOOs drastically emerge in association with glass transition. Furthermore, the segments composed of LBOOs apparently have lower mobility than that of other segments and their duration time are upheld until approximately three times τ_α. These results strongly indicate that LBOOs are the origin of dynamic heterogeneity. This result supports the concept of "frustration to crystallization" as a physical picture of glass transition in two-order-parameter model.[45,46] One interesting fact is that orders we have found which distinguish glass state are found in coarse grained space. Although many researches have been conducted over the years to find any structures which distinguish glass state in polymer, nothing has ever been found. This may be because LBOOs are only observed in coarse grained space. Furthermore, from the results that segments composed of LBOOs are concertedly vibrating in the direction of orientation bond, we indicated the possibility that LBOOs can be identified as CRR. It means that we could prove that LBOOs we found are consistent with both the physical picture of "frustration to crystallization" and Adam−Gibbs' picture. At least in polymer glass, we can interpret that two-order-parameter model gives theoretical background of forming local crystalline orders when approaching T_g and Adam−Gibbs theory gives explanation to the mechanism of extreme slow down of dynamics and dynamic heterogeneity caused by local crystalline orders. Note that our results were obtained in a general model for straight-chain polymers, which was the most representative glass-forming liquid. Our results may lead to further understanding of other glass-forming liquids.

APPENDIX. TWO-BONDS-CORRELATION-FUNCTION

Given a bond (bond 2) is inclined at an angle of θ to a certain bond (bond 1) at distance L, bond 2 is free to rotate about an axis of bond 1 maintaining an angle of θ. Moreover, bond 2 is also free to rotate about the axis which is parallel to bond 1 and passing through the midpoint of bond 2. Then, the existence probability $P_1(L,\theta)$ of bond 2 for bond 1 is proportionate to passing area of segment connecting to bond 2. Therefore, we define $P_1(L,\theta)$ as follows:

$$P_1(L,\theta) = \frac{2\pi Lb \sin\theta}{\int 2\pi Lb \sin\theta \, d\theta} = \sin\theta \tag{A1}$$

Here, b is the bond length and $0° \le \theta \le 90°$. When the number of bonds with L and θ is measured as $\phi_i(L,\theta)$, its existence probability $P_2(L,\theta)$ is expressed as A2.

$$P_2(L,\theta)^2 = \frac{\langle\phi(L,\theta)\rangle}{\int \langle\phi(L,\theta)\rangle \, d\theta} \tag{A2}$$

dx.doi.org/10.1021/ma201341d |*Macromolecules* 2011, 44, 6615–6624

We define $\psi(L,\theta)$ as the proportion of $P_2(L,\theta)$ to $P_1(L,\theta)$.

$$\psi(L,\theta) = \frac{\langle \phi_i(L,\theta)\rangle}{\sin\theta \int \langle \phi_i(L,\theta)\rangle \, d\theta} \quad \text{(A3)}$$

■ ACKNOWLEDGMENT

We thank H. Morita, E. Nihei, Y. Fujitani, O. Yamamuro, H. Takano, and T. Kawakatsu for fruitful discussions. We also thank M. Kojima for her technical advice in writing this manuscript. This research is supported by a Grant-in-Aid for the Japan Society for the Promotion of Science (JSPS) Fellows and JSPS through its "Funding Program for World-Leading Innovative R&D on Science and Technology (FIRST Program)." A grant of computer time at information technology center of Keio University is gratefully acknowledged.

■ REFERENCES

(1) Angell, C. A. Relaxation in liquids, polymers and plastic crystals—strong/fragile patterns and problem. *J. Non-Cryst. Solids* **1991**, *13*, 131–133.

(2) Debenedetti, P. G.; Stillinger, F. H. Supercooled liquids and the glass transition. *Nature* **2001**, *410*, 259–267.

(3) Jackle, J. Models of the glass transition. *Rep. Prog. Phys.* **1986**, *49*, 171–231.

(4) McKenna, G. B. *Comprehensive Polymer Science*; Pergamon: Oxford, U.K., 1989.

(5) Donth, E. W. *The Glass Transition: Relaxation Dynamics in Liquids and Disordered Materials*; Springer: Berlin, 2001.

(6) Angell, C. A. Entropy and fragility in supercooling liquids. *J. Res. Natl. Inst. Stand. Technol.* **1997**, *102*, 171–185.

(7) Andersen, H. C. Molecular dynamics studies of heterogeneous dynamics and dynamic crossover in supercooled atomic liquids. *Proc. Natl. Acad. Sci. U.S.A.* **2005**, *102*, 6686–6691.

(8) Starr, F. W.; Sastry, S.; Douglas, J. F.; Glotzer, S. What Do We Learn from the Local Geometry of Glass-Forming Liquids? *Phys. Rev. Lett.* **2002**, *89*, 125501.

(9) Bordat, P.; Affouard, F.; Descamps, M.; Ngai, K. L. Does the Interaction Potential Determine Both the Fragility of a Liquid and the Vibrational Properties of Its Glassy State? *Phys. Rev. Lett.* **2004**, *93*, 105502.

(10) Widmer-Cooper, A.; Harrowell, P. Predicting the Long-Time Dynamic Heterogeneity in a Supercooled Liquid on the Basis of Short-Time Heterogeneities. *Phys. Rev. Lett.* **2006**, *96*, 185701.

(11) Ediger, M. D. Spatially Heterogeneity Dynamics in Supercooled Liquids. *Annu. Rev. Phys. Chem.* **2000**, *51*, 99–128.

(12) Richert, R. Heterogeneous dynamics in liquids: fluctuations in space and time. *J. Phys.: Condens. Matter* **2002**, *14*, R703–R738.

(13) Scopigno, T.; Ruocco, G.; Sette, F.; Monaco, G. Is the Fragility of a Liquid Embedded in the Properties of Its Glass? *Science* **2003**, *302*, 849–852.

(14) Novikov, V. N.; Sokolov, A. P. Poisson's ratio and fragility of glass-forming liquids. *Nature* **2004**, *431*, 961–963.

(15) Onuki, A., Furukawa, A., Minami, A.Presented at Stat-Phys 22, Bangalore, India, July 4−9, 2004.

(16) Gotze, W. In *Liquids, Freezing, and the Glass Transition*; Hansen, J. P., Levesque, D., Zinn-Justin,J., Eds.; North-Holland: Amsterdam, 1991.

(17) Liu, A. J.; Nagel, S. R. Jamming is not just cool any more. *Nature* **1998**, *396*, 21–22.

(18) Coluzzi, B.; Parisi, G.; Verrocchio, P. Thermodynamical Liquid-Glass Transition in a Lennard-Jones Binary Mixture. *Phys. Rev. Lett.* **2000**, *84*, 306–309.

(19) Allen, M. P., Tildesley, D. J. *Computer Simulation of Liquids*; Clarendon: Oxford, U.K., 1987.

(20) Rapaport, D. C. *The Art of Molecular Dynamics Simulation*; Academic: San Diego, CA, 1996.

(21) *Monte Carlo and Molecular Dynamics of Condensed Matter System*; Binder, K., Ciccotti, G., Eds.; Societa Italiana di Fisica: Bologna, Italy, 1996.

(22) Shintani, H.; Tanaka, H. Frustration on the way to crystallization in glass. *Nature Phys* **2006**, *2*, 200–206.

(23) Kawasaki, T.; Araki, T.; Tanaka, H. Correlation between Dynamic Heterogeneity and Medium-Range Order in Two-Dimensional Glass-Forming Liquids. *Phys. Rev. Lett.* **2007**, *99*, 215701.

(24) Kanaya, T.; Buchenau, U.; Kiozumi, S.; Tsukushi, I.; Kaji, K. Non-Gaussian behavior of crystalline and amorphous phases of polyethylene. *Phys. Rev. B* **2000**, *61*, R6451–R6454.

(25) Kremer, K.; Grest, G. S. Dynamics of entangled linear polymer melts: A molecular − dynamics simulation. *J. Chem. Phys.* **1990**, *92*, 5057–5086.

(26) Larini, L.; Ottochian, A.; De Michele, C.; Leporini, D. Universal scaling between structural relaxation and vibrational dynamics in glass-forming liquids and polymers. *Nature Phys* **2008**, *4*, 42–45.

(27) Baschnagel, J.; Bennemann, C.; Paul, W.; Binder, K. Dynamics of a supercooled polymer melt above the mode-coupling critical temperature: cage versus polymer-specific effects. *J Phys: Condens Matter* **2000**, *12*, 6365–6374.

(28) Buchholz, J.; Paul, W.; Varnik, F.; Binder, K. Cooling rate dependence of the glass transition temperature of polymer melts: Molecular dynamics study. *J. Chem. Phys.* **2002**, *117*, 7364–7372.

(29) Bennemann, C.; Paul, W.; Binder, K.; Dunweg, B. Molecular-dynamics simulations of the thermal glass transition in polymer melts: α-relaxation behavior. *Phys. Rev. E* **1998**, *57*, 843–851.

(30) Bennemann, C.; Baschnagel, J.; Paul, W. Molecular-dynamics simulation of a glassy polymer melt: Incoherent scattering function. *Eur. Phys. J. B* **1999**, *10*, 323–334.

(31) Aichele, M.; Baschnagel, J. Glassy dynamics of simulated polymer melts: Coherent scattering and van Hove correlation functions - Part II: Dynamics in the α-relaxation regime. *Eur. Phys. J. E* **2001**, *229*, 245–256.

(32) Bennemann, C.; Baschnagel, J.; Paul, W.; Binder, K. Molecular-dynamics simulation of a glassy polymer melt: Rouse model and cage effect. *Comput. Theor. Polym. Sci.* **1999**, *9*, 217–226.

(33) Bennemann, C.; Donati, C.; Baschnagel, J.; Glotzer, S. C. Growing range of correlated motion in a polymer melt on cooling towards the glass transition. *Nature* **1999**, *399*, 246–249.

(34) Nose, S. A molecular dynamics method for simulations in the canonical ensemble. *Mol. Phys.* **1984**, *52*, 255–268.

(35) Nose, S. A unified formulation of the constant temperature molecular dynamics methods. *J. Chem. Phys.* **1984**, *81*, 511–519.

(36) Andersen, H. C. Molecular dynamics simulations at constant pressure and/or temperature. *J. Chem. Phys.* **1980**, *72*, 2384–2393.

(37) Vogel, H. Das Temperaturabhängigkeitsgesetz der Viskosität von Flüssigkeiten. *Phys Z.* **1921**, *22*, 645–646.

(38) Fulcher, G. S. Analisis of Recent Measurements of the Viscosity of Glass. *J. Am. Ceram. Soc.* **1925**, *8*, 339–355.

(39) Tammann, G. On Glasses as Supercooled Liquids. *J. Soc. Glass Technol.* **1925**, *9*, 166–184.

(40) Hecksher, T.; Nielsen, A. I.; Olsen, N. B.; Dyre, J. C. Little evidence for dynamic divergences inultraviscous molecular liquids. *Nature Phys.* **2008**, *4*, 737–741.

(41) Perera, D. N.; Harrowell, P. Stability and structure of a supercooled liquid mixture in two dimensions. *Phys. Rev. E* **1999**, *59*, 5721–5734.

(42) Kegel, W. K.; van Blaaderen, A. Direct Observation of Dynamical Heterogeneities in Colloidal Hard-Sphere Suspensions. *Science* **2000**, *287*, 290–293.

(43) Kob, W.; Donati, C.; Plimpton, S. J.; Poole, P. H.; Glotzer, S. C. Dynamical Heterogeneities in a Supercooled Lennard-Jones Liquid. *Phys. Rev. Lett.* **1997**, *79*, 2827–2830.

(44) Adam, G.; Gibbs, J. H. On the Temperature Dependence of Cooperative Relaxation Properties in Glass − Forming Liquids. *J. Chem. Phys.* **1965**, *43*, 139–146.

(45) Tanaka, H. Two-Order-Parameter Description of Liquids: I. A General Model of Glass Transition Covering its Strong to Fragile Limit. *J. Chem. Phys.* **1999**, *111*, 3163–3174.

(46) Tanaka, H. Two-Order-Parameter Description of Liquids: II. Criteria for Vitrification and Predictions of Our Model. *J. Chem. Phys.* **1999**, *111*, 3175–3182.